HETEROCYCLES, Vol. 100, No. 11, 2020, pp. 1845 - 1858. © 2020 The Japan Institute of Heterocyclic Chemistry
Received, 22nd July, 2020, Accepted, 26th August, 2020, Published online, 3rd September, 2020
DOI: 10.3987/COM-20-14327

SYNTHESIS AND EVALUATION OF BIOLOGICAL PROPERTIES OF 2-(2-(PHENOXY)PYRIDIN-3-YL)QUINAZOLIN-4(3*H*)-ONE DERIVATIVES

Li-qiong Zhang,[1#] Jia-min Liu,[1#] Yi-yuan Gan,[1] Li-hui Shao,[1] Yi-hong Fu,[1] Zhen-chao Wang,[1,2*] and Gui-ping Ouyang[1,2,3*]

[1] College of Pharmacy, Guizhou University, Guiyang, 550025, P. R. China; [2] State Key Laboratory of Functions and Applications of Medicinal Plants, Guizhou Medical University, Guiyang, 550014, P. R. China; [3] Guizhou Engineering Laboratory for Synthetic Drugs, Guizhou University, Guiyang, 550025, P. R. China. [#] These authors contributed equally to this work. Email: wzc.4884@163.com, gpouyang@gzu.edu.cn.

Abstract – A series of novel 2-(2-(phenoxy)pyridin-3-yl)quinazolin-4(3*H*)-one derivatives were designed, synthesized as antitumor agents. The antitumor activities of target compounds were evaluated and compared with positive drug Gefitinib employing standard MTT assay against A549 (human lung adenocarcinoma cell), PC-3 (prostate cancer cells), K562 (human chronic myeloid leukemia cells), HepG2 (human liver cancer cell) cancer cell lines *in vitro*. The pharmacological screening results revealed that many compounds exhibited moderate levels of antitumor activities against four cancer cell lines, especially 6-chloro-2-(2-(3,5-dimethylphenoxy)pyridin-3-yl)-3,8-dimethylquinazolin-4(3*H*)-one (**z8**) displayed promising activities against A549 (IC_{50} = 12.47±2.86 μM) than Gefitinib (IC_{50} = 17.37±6.01 μM). The mechanism and the apoptosis inducing effect of **z8** against A549 cell line were studied. The results showed that **z8** could inhibit migration and motility of cancer cells, induce cell apoptosis and exhibit the typical apoptotic morphology.

INTRODUCTION

Cancer is a major public health problem worldwide causing the second-highest mortality rate after cardiovascular diseases. The American Cancer Society estimates that prostate cancer, lung and bronchial cancer, and colorectal cancer (CRC) are the most common cancers expected to be diagnosed in men and

women in the United States in 2019. These cancers accounted for 42% of all newly diagnosed cancer cases in men with prostate cancer accounting for one fifth.[1] To date, the current treatment for the cancer is through chemotherapy, radiation, surgery, biological, and hormonal.[2]

The biological activities of 4-aminoquinazolines have been demonstrated as kinase inhibitors including EGFR (epidermal growth factor receptor),[3] EGFR/VEGFR (epidermal growth factor receptor/vascular endothelial growth factor receptor),[4] HER2 (human epidermal growth factor receptor 2), VEGFR,[5,6] RET (rearranged during transfection),[7,8] and PI3K (phosphoinositide 3-kinases).[9,10] And some of the drugs with 4-aminoquinazoline core are already in the market such as Erlotinib, Gefitinib, Afatinib, Decomitinib, etc. However an increasing number of studies showed that quinazolinone derivatives are of considerable pharmacological chemicals as anticancer agents. Quinazolinone derivatives are significant class of nitrogen-rich heterocyclic compounds, as this moiety is present in a variety of bioactive natural products, synthetic drugs, agrochemicals, and pharmaceuticals. Quinazolinone conjugated amino acid **a** (Figure 1, **a**) showed excellent anticancer activity against the tested human MDA-MB-231 (human triple negative breast cancer cells), A549 (non-small cell lung cancer), and MCF7 (melanoma cell lines) cancer cell lines with the compound bonded effectively to DNA.[11] Compound **b** (Figure 1, **b**) exhibited the remarkable PI3Kδ inhibitory activity with IC_{50} value of 6.3 nM. Consistent with the potent enzymatic activity, **b** also exerted the most favorable cytotoxic efficacy against SU-DHL-6 (human malignant B-cell line) cell line with GI_{50} value of 0.21 μM.[12] Quinazolinone derivative **c** (Figure 1, **c**) showed a submicromolar range as a potential Hedgehog pathway inhibitors (IC_{50} = 0.038 nM).[13] The hydrazone structure such as the compound **d** has special biological activity due to its strong coordination ability and various coordination modes.

Through our research, we found some hydrazone derivatives have good activity against plant pathogens.[14] Moreover, compound **e** is a possible anticancer drug molecule due to its good binding and inhibitory effect on $EGFR^{wt}$-TK (wild type epidermal growth factor receptor tyrosine kinase).[15] The rigid cyclized structure of quinazolinone derivatives may lead to better binding affinity and pharmacokinetics of the parent drug candidate.[13] In order to further explore the biologically active quinazolinone compounds, we introduced a pyridyl group in the structure of quinazolinone and combined phenoxy groups with different substituents into the molecule to obtain a series of relatively rigid compound. In this study, a class of quinazolinone derivatives containing 2-(2-(phenoxy)pyridin-3-yl)quinazolin-4(3*H*)-one were synthesized. Further, the anticancer properties of the target molecules were evaluated against human tumor cell lines including A549, PC-3 (prostate cancer cells), HepG2 (hepatocellular carcinoma), K562 (human chronic granulocytic leukemia). In addition, we further studied the characteristics of the compounds on the migration and apoptosis of cancer cells.

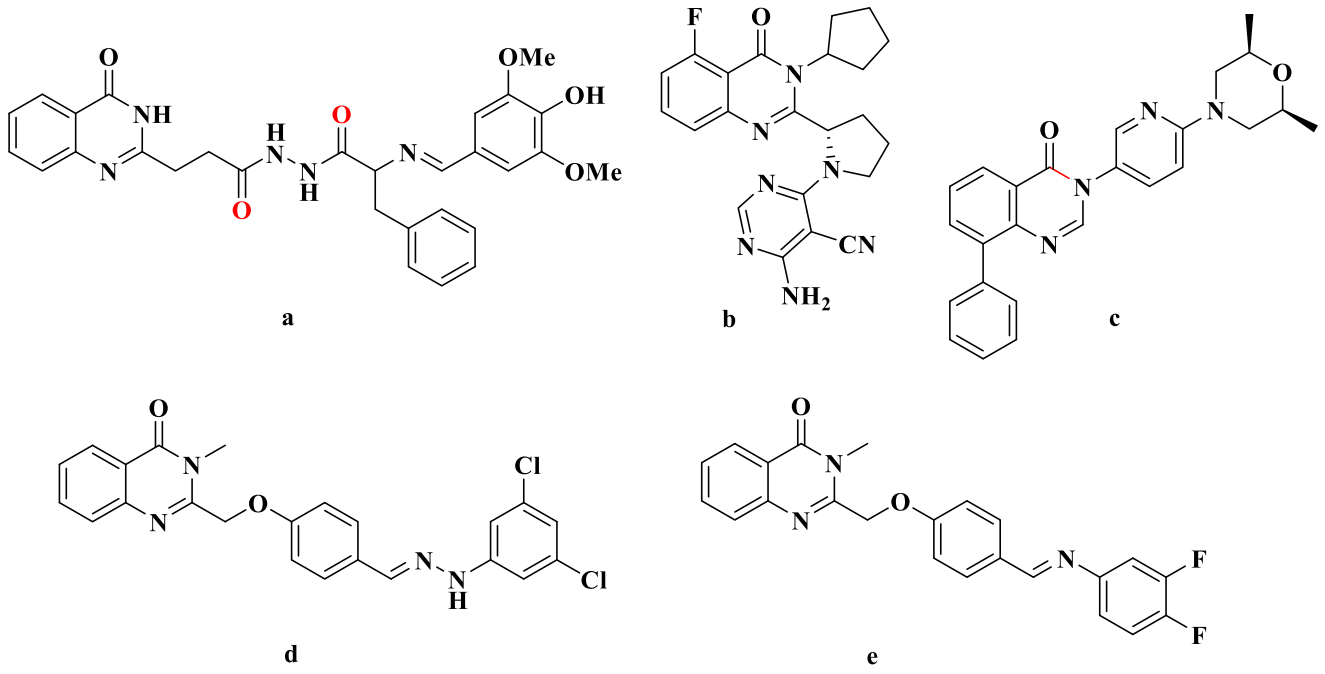

Figure 1. Structures of reported anticancer quinazolinones and biologically active quinazolinone compounds

RESULTS AND DISCUSSION

The most common and practical synthetic methods for quinazolinone are oxidative heterocyclization of *o*-aminobenzamides with aldehydes[16] or one-pot synthesis of quinazolinones between primary alcohols or benzyl alcohols and *o*-aminobenzamides via dehydrogenations under catalytic conditions.[17,18] In addition, it has been reported in the literature that the synthesis of quinazolinone cores usually uses inexpensive and readily available substituted 2-halobenzamides and methylamines (or aryl),[19,20] or uses anthranilic acid as a starting material.[21] The synthesis of quinazolinone usually involves a cyclization reaction between two molecules, and the intramolecular cyclization reaction may require a higher heating temperature.[22]

Recently, our group have developed an interesting procedure for the synthesis of 2-pyridyl substituted quinazolinone core by the reaction of 2-amino-5-chloro-*N*,3-dimethylbenzamide (**m**) with 2-chloronicotinoyl chloride (**2**) under catalyst free conditions in two steps with good to excellent yields. Firstly, the starting materials 2-chloronicotinic acid (**1**) and $SOCl_2$ were refluxed under anhydrous conditions using DMF as a catalyst to acylate into 2-chloronicotinoyl chloride **2**. After removing excess $SOCl_2$ under reduced pressure, the product can be used in the next synthesis without purification (Yield 94%). Next, **2** was dissolved in CH_2Cl_2 and added dropwise to the suspension of 2-amino-5-chloro-*N*, 3-dimethylbenzamide and K_2CO_3 in CH_2Cl_2 under ice bath conditions. After stirring at 0 °C for 2 hours, the temperature was raised to room temperature to continue the reaction, and

intermediate **3** was obtained (Yield 84%). Then intermediate **3** was dissolved in DMF and heated to 115 °C under alkaline conditions provided by K_2CO_3. Obviously, intermediate **3** was easy to undergo intramolecular ring-closure reaction to obtain the desired pyridyl substituted quinazolinone core. TLC monitored the reaction until intermediate **3** was consumed and intermediate **4** was obtained (Yield 85%). Subsequently a nucleophilic substitution reaction between phenol (**x**) and 2-chloropyridine part (**4**) was then used to obtain the desired products (Scheme 1). The target products **z1**−**z14** were synthesized by dissolving compound **4** and phenols **x** in NMP, using Cs_2CO_3 to provide basic conditions and as a catalyst, and heating to 130 °C to successfully perform nucleophilic substitution reaction of phenols **x** and 2-chloropyridine. The structures of compounds **z1**−**z14** are confirmed by spectral data.

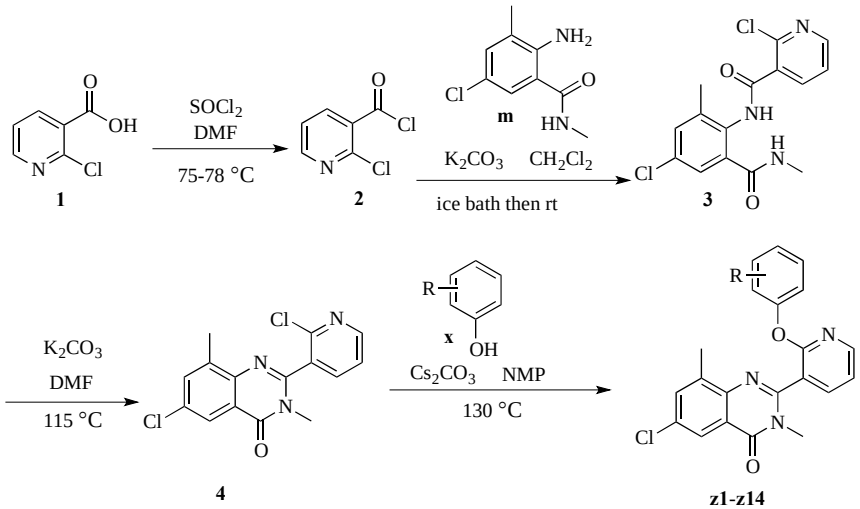

z1, R = 3, 4-dichloro
z2, R = 3, 5-dichloro
z3, R = 4-fluoro
z4, R = 3,4-difluoro
z5, R = 4-iodo
z6, R = 3, 4-dimethyl
z7, R = 3-chloro-4-fluoro
z8, R = 3,5-dimethyl
z9, R = 3-trifluoromethyl
z10, R = 3-fluoro
z11, R = 4-chloro-3-methyl
z12, R = 2-fluoro
z13, R = 3-bromo
z14, R = 4-fluoro-2-methyl

Scheme 1. Synthesis of target compounds

The anticancer activity of synthetic compounds *in vitro* against four human cancer cell lines was evaluated by the MTT assay, including A549, PC-3, HepG2 and K562. Cell cytotoxicity assay was carried out using the same way. We found that several compounds have good anticancer activity, and all compounds have no toxic effect on normal cells. From the data in Table 1, we found that compounds **z4**, **z7**, **z8**, and **z9** inhibited the growth of PC-3 cells (27.88 ± 5.97%, 31.28 ± 3.96%, 30.54 ± 8.35% and 30.96 ± 7.20%, respectively) similar to the positive control drug Gefitinib (31.81 ± 1.80%). The different substituents on the benzene ring showed moderate to good activity with 9.92 to 31.81% inhibition rate towards PC-3 when treated at 10 μM concentration. When analyzing the activity of all compounds on

PC-3, we found that compounds with two electron-withdrawing groups as substituent had better activity, and *m*-trifluoromethyl was an effective substituent. The activity of the compounds was as follows: **z7** (3-chloro-4-fluoro) > **z9** (3-trifluoromethyl) > **z4** (3,4-difluoro) > **z1** (3,4-dichloro). When the substituents were two electron-donating groups and the positions were different, the activity of the compound was obviously different. For example, the inhibitory activity of **z8** (3,5-dimethyl) on three cancer cells (A549, PC-3, HepG2) was obviously stronger than that of **z6** (3,4-dimethyl). Interestingly, the activities of compounds **z7**, **28** and **z9** on A549 were also significantly better than other compounds, and the order of inhibition rate was **z8** > **z9** > **z7**. Herein, we tested the IC_{50} values of compounds **z7**, **z8** and **z9** on four cancer cells, and the result was listed in Table 2.

We discovered that **z8** was the lead compound with the best growth inhibitory activity on A549, PC-3 and HepG2 cell lines among the tested compounds. The inhibitory activity of **z8** against A549 was superior to the positive control Gefitinib (17.37 ± 6.01 μM) with IC_{50} value of 12.47 ± 2.86 μM. And the IC_{50} value of **z8** for PC-3 and HepG2 was 16.27 ± 6.84 μM (Gefitinib, 9.95 ± 2.13 μM) and 16.48 ± 2.04 μM (Gefitinib, 16.94 ± 7.53 μM). The results indicated that **z8** was the most active anticancer compound in this series of compounds.

Given the importance of cell migration in pathobiology of cancer, we have investigated the effect of compound **z8** on A549 cells by performing wound scratch assay. As depicted in Figure 2, it was observed that artificially created wound was closed in control cells reflecting the rapid proliferation and migratory property of cancer cells. Furthermore, **z8** treated cells showed significant inhibition of cell migration into the wound area. A concentration dependent effect was observed where the low dose (10 μM) showed partial closure of the denuded area, mid dose (20 μM) treatment showed wound mild closure where as the highest dose of 30 μM displayed conspicuous suppression of cell migration as evident from the scantly present cells in the denuded area. These results suggested the potential of **z8** inhibition migration and motility of cancer cells.

A549 cells treated with compound **z8** at 5 to 30 μM for 48 hours were stained with DAPI, and A549 cells not treated with the **z8** were used as control. The results were given in Figure 3. Additionally, condensed chromosome and nuclear fragmentation were apparent in apoptotic cells. The results from the Figure 3 clearly demonstrated that the nuclear structure of untreated cells showed normal round nuclei whereas **z8** treated cells exhibited nuclear fragmentation, condensed chromosome and the characteristic pyknotic, horse shoe pattern of the nuclei. The high concentration treated cells showed higher degree of apoptosis as evidenced by the increased number of horseshoe shaped nuclei.

Table 1. Antitumor studies of synthesized compounds

compds	*In vitro* inhibition rate (%)[a]			
	A549	PC-3	HepG2	K562
z1	4.67±7.38	25.04±1.83	6.05±3.95	31.71±5.80
z2	5.89±4.38	20.6±3.45	10.08±4.50	28.39±4.00
z3	5.74±3.66	20.79±10.29	11.88±8.36	17.67±11.55
z4	12.86±3.18	27.88±5.97	4.43±4.19	12.52±2.16
z5	17.07±3.45	16.36±5.98	13.28±1.89	15.09±1.37
z6	2.48±6.58	16.52±13.34	12.29±0.11	8.55±5.08
z7	15.39±5.76	31.28±3.96	17.25±3.63	11.82±3.70
z8	26.91±3.30	30.54±8.35	18.21±12.48	8.39±3.33
z9	19.69±4.47	30.96±7.20	5.58±2.33	9.44±7.43
z10	9.62±2.14	15.55±12.29	6.92±7.93	8.04±6.37
z11	2.70±6.63	9.92±5.78	1.12±1.32	4.29±4.99
z12	14.58±0.51	16.88±2.83	19.95±4.41	11.65±10.95
z13	7.14±7.11	12.97±1.68	16.4±2.94	8.10±1.42
z14	9.48±4.98	17.09±3.99	15.07±2.45	17.00±4.50
Gefitinib	28.68±5.03	31.81±1.80	28.18±7.44	30.51±5.41

[a)] Inhibition rate measured at a drug concentration of 10 μM.

Table 2. Cytotoxic activities of compounds against four cancer cells

compds	*In vitro* cytotoxicity of IC_{50}[a]			
	A549	PC-3	HepG2	K562
z7	19.4±3.11	20.36±7.18	34.91±11.77	24.14±6.02
z8	12.47±2.86	16.27±6.84	16.48±2.04	30.27±0.25
z9	19.76±6.46	23.70±4.98	24.35±9.54	40.22±0.69
Gefitinib	17.37±6.01	9.95±2.13	16.94±7.53	24.14±6.02

[a)] Growth inhibitory activity was tested with compound concentrations diluted in gradients. IC_{50} values determined from the dose response curve were expressed in μM. The IC_{50} are presented as mean values of three independent experiments done in quadruplicates. Coeffificients of variation were < 10% in all cases.

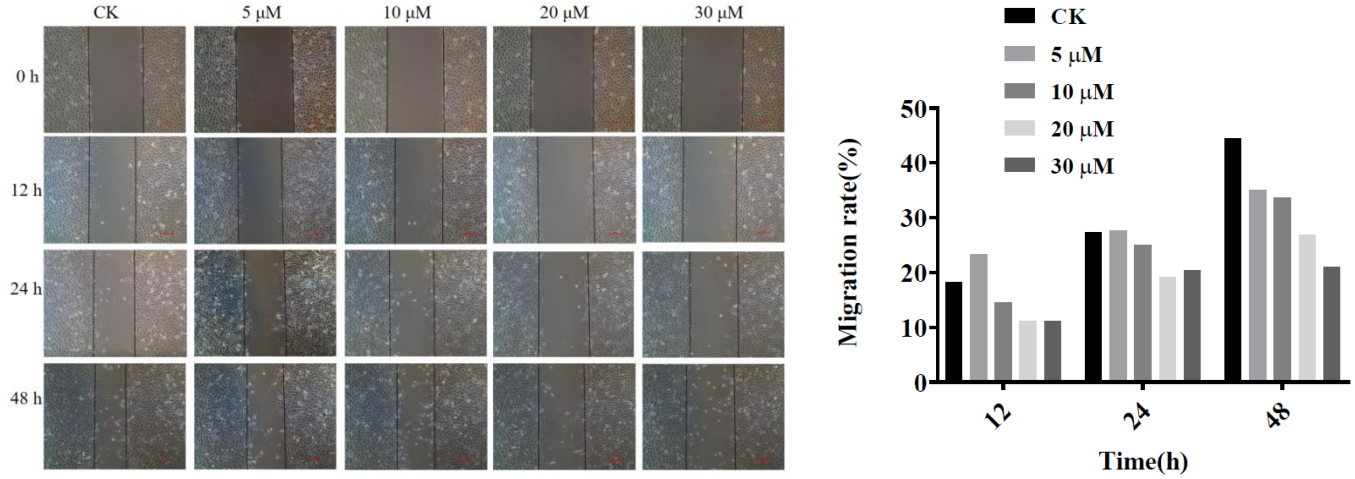

Figure 2. Representative microphotographs of cell migration assay of all experimental groups from 0 h to 48 h (Magnification 10×). Treated wells show reduction in migration of cells into the artificially created wound. Graphical representation of inhibition in cell migration upon treatment with **z8** at different concentration.

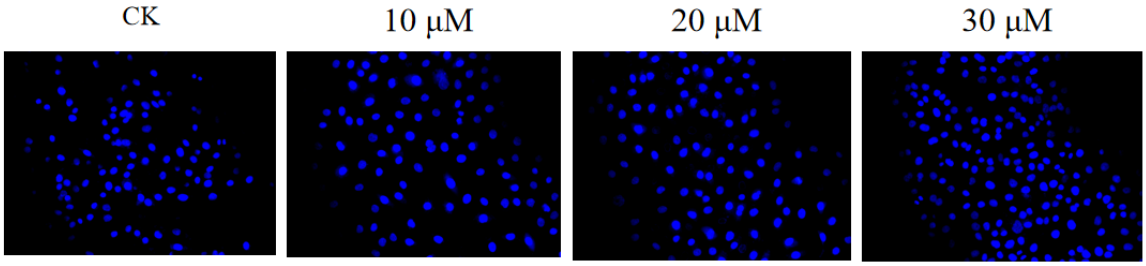

Figure 3. Representative microphotographs of morphological changes in nuclei of untreated cells and as a result of treatment with **z8** in A549 cells as indicated by DAPI staining (Magnification 20×).

In conclusion, a series of quinazolin-4(3*H*)-one derivatives were synthesized. Among all the tested compounds, compound **z8** is the best anticancer compound against A549 and HepG2 cell lines in this series of compounds and showed significant inhibition of cell migration into the wound area. As well, it induced cell apoptosis and exhibited typical apoptotic morphology in a dose dependent manner. These results indicated that **z8** is a promising antitumor agent among these compounds.

EXPERIMENTAL

Chemistry

All commercial reagents are analytically pure and used without further purification. Nuclear magnetic resonance (NMR) spectra were recorded on a JEOL-ECX 500 NMR spectrometer operating at 500 and 126 MHz at room temperature or JEOL-ECX 400 NMR spectrometer operating at 400 and 101 MHz at room temperature. ^{1}H NMR chemical shifts (δ) were referenced to internal standard tetramethylsilane (for ^{1}H, δ = 0.00 ppm). ^{13}C NMR chemical shifts were referenced to internal solvent $CDCl_3$ (for ^{13}C, δ = 77.16

ppm). High-resolution mass spectrometry (HRMS) spectra were recorded on a high-resolution magnetic sector mass spectrometer with an electrospray ionization (ESI) source. Melting points were determined on an XT-4 binocular microscope (Beijing Tech Instrument Co., Beijing, China) and uncorrected.

All reactions were carried out in oven-dried flasks with magnetic stirring. All the experiments were monitored by analytical thin-layer chromatography (TLC) performed on silica gel GF254 pre-coated plates. All commercial reagents are analytically pure and used without further purification.

General procedure for preparing compound 2

Intermediate **2** was synthesized according to reported method in reference with slight modifications.[23] A suspension of 2-chloronicotinic acid (5 g, 31.74 mmol) and DMF (0.23 g, 3.17 mmol) in thionyl chloride (35 mL) was refluxed in moisture-free conditions with $CaCl_2$ as desiccant for 6−8 h. After the reaction was completed, $SOCl_2$ was distilled off under reduced pressure, and (20 mL×2 times) CH_2Cl_2 was added to distill again to completely remove $SOCl_2$ to obtain a brown-yellow solid. The product was used in the next step without purification (5.25 g, yield 94%).

General procedure for preparing compound 3

To a solution of 2-amino-5-chloro-*N*, 3-dimethylbenzamide (225.74 mg, 1.14 mmol), and K_2CO_3 (78.53 mg, 0.57 mmol) in dry CH_2Cl_2 (40 mL), **2** (200 mg, 1.14 mmol) dissolved in dry CH_2Cl_2 (10 mL) was added drop-wise using a pressure equalizing funnel. The mixture was allowed to stir at 0 °C temperature for 2 h then 24 h at room temperature. TLC monitors the reaction until **2** was consumed. The reaction mixture was poured into the ice water (100 mL). Then the product was filtered, washed with water and dried, recrystallized from EtOH affording the pure **3** (322.82 mg, yield 84%).

General procedure for preparing compound 4

A suspension of intermediate **3** (3.0 g, 8.87 mmol), K_2CO_3 (2.45 g, 17.74 mmol) and 15 mL of DMF was stirred for 10 min, and then heated to 115 °C for reaction. TLC monitored reaction until intermediate **3** consumed. The reaction was completed about 25 h. The slurry was poured into ice water (80 mL), and the white solid was filtered, washed with a small amount of water, dried, and then recrystallized from anhydrous EtOH to obtain white powder **4** (2.79 g, yield 98%).

General procedure for preparing compound z1−z14

Compound **4** (0.6 g, 1.87 mmol), Cs_2CO_3 (1.22 g, 3.75 mmol), 8 mL NMP and *p*-iodophenol (1.03 g, 4.68 mmol) were sequentially added to a 50 mL round bottom flask. Stirred for 10 min and then heated to 130 °C. Raw material **4** was monitored by TLC until it consumed. After the slurry was cooled, the reaction mixture was poured into 40 mL ice water while stirring, and then filtered under reduced pressure, and washed with 20 mL of water and 10 mL of EtOH in order. Dried and dissolved it in heated EtOAc (40 mL×3 times). After the solution was clear, the supernatant was decanted. The supernatant was collected and filtered through a pad of silica gel. The solvent was recovered under reduced pressure, and the crude

product was recrystallized from petroleum ether/EtOH (v:v = 2:1). After filtration, the solid phase was recrystallized from dioxane/petroleum ether (v:v = 1:2). If necessary, repeat the recrystallization twice. **z5** (0.48 g, yield 51%).

Characterization 6-Chloro-2-(2-(3,4-dichlorophenoxy)pyridin-3-yl)-3,8-dimethylquinazolin-4(3*H*)-one (z1). Yield: 32.1%, white powder, mp 159.4–161.3 °C; ^{1}H NMR (500 MHz, $CDCl_3$) δ 8.31 (d, *J* = 3.4 Hz, 1H), 8.13 (s, 1H), 7.96 (d, *J* = 7.2 Hz, 1H), 7.55 (s, 1H), 7.44 (d, *J* = 8.7 Hz, 1H), 7.27 (d, *J* = 2.4 Hz, 1H), 7.25 (d, *J* = 2.3 Hz, 1H), 7.01 (dd, *J* = 8.7, 2.4 Hz, 1H), 3.55 (s, 3H), 2.56 (s, 3H). ^{13}C NMR (101 MHz, $CDCl_3$) δ 161.62, 159.29, 151.64, 150.87, 149.22, 144.69, 140.43, 138.55, 135.03, 133.16, 132.61, 130.92, 129.16, 123.77, 123.64, 121.78, 121.20, 120.17, 119.59, 33.01, 17.31. HRMS (ESI) *m/z* calcd for $C_{21}H_{15}O_2N_3Cl_3$ $[M+H]^+$ 446.0224, found 446.0218.

6-Chloro-2-(2-(3,5-dichlorophenoxy)pyridin-3-yl)-3,8-dimethylquinazolin-4(3*H*)-one (z2). Yield: 40.0%, white powder, mp 195.1–197.0 °C; ^{1}H NMR (500 MHz, $CDCl_3$) δ 8.34 (d, *J* = 3.4 Hz, 1H), 8.13 (s, 1H), 7.96 (d, *J* = 6.4 Hz, 1H), 7.55 (s, 1H), 7.27 (dd, *J* = 6.9, 5.5 Hz, 1H), 7.20 (s, 1H), 7.07 (s, 2H), 3.54 (s, 3H), 2.55 (s, 3H). ^{13}C NMR (101 MHz, $CDCl_3$) δ 161.62, 159.29, 151.64, 150.87, 149.22, 144.69, 140.43, 138.55, 135.03, 133.16, 132.61, 130.92, 129.16, 123.77, 123.64, 121.78, 121.20, 120.17, 119.59, 33.01, 17.31. HRMS (ESI) *m/z* calcd for $C_{21}H_{15}O_2N_3Cl_3$ $[M+H]^+$ 446.0224, found 446.0218.

6-Chloro-2-(2-(4-fluorophenoxy)pyridin-3-yl)-3,8-dimethylquinazolin-4(3*H*)-one (z3). Yield: 32.3%, white powder, mp 181.6–183.4 °C; ^{1}H NMR (400 MHz, $CDCl_3$) δ 8.22 (d, *J* = 6.3 Hz, 1H), 8.06 (s, 1H), 7.86 (d, *J* = 8.8 Hz, 1H), 7.49 (s, 1H), 7.13 (dd, *J* = 7.2, 5.1 Hz, 1H), 7.03 (d, *J* = 9.2 Hz, 2H), 7.00 (d, *J* = 3.2 Hz, 2H), 3.51 (s, 3H), 2.50 (s, 3H). ^{13}C NMR (101 MHz, $CDCl_3$) δ 161.68, 161.14, 160.00, 158.70, 151.31, 149.25, 148.63, 144.78, 140.26, 138.52, 134.96, 132.50, 123.64, 123.04, 121.80, 119.97, 118.97, 116.48, 116.25, 33.00, 17.33. HRMS (ESI) *m/z* calcd for $C_{21}H_{16}O_2N_3ClF$ $[M+H]^+$ 396.0910, found 396.0904.

6-Chloro-2-(2-(3,4-difluorophenoxy)pyridin-3-yl)-3,8-dimethylquinazolin-4(3*H*)-one (z4). Yield: 22.8%, white powder, mp 166.4–167.4 °C; ^{1}H NMR (500 MHz, $CDCl_3$) δ 8.31 (d, *J* = 6.7 Hz, 1H), 8.13 (s, 1H), 7.95 (d, *J* = 9.1 Hz, 1H), 7.55 (s, 1H), 7.24 (dd, *J* = 7.4, 5.1 Hz, 1H), 7.17 (dd, *J* = 18.5, 9.1 Hz, 1H), 7.01 (dd, *J* = 10.5, 6.8 Hz, 1H), 6.87 (d, *J* = 8.8 Hz, 1H), 3.56 (s, 3H), 2.56 (s, 3H). ^{13}C NMR (101 MHz, $CDCl_3$) δ 161.62, 159.29, 151.64, 150.87, 149.22, 144.69, 140.43, 138.55, 135.03, 133.16, 132.61, 130.92, 129.16, 123.77, 123.64, 121.78, 121.20, 120.17, 119.59, 33.01, 17.31. HRMS (ESI) *m/z* calcd for $C_{21}H_{15}O_2N_3ClF_2$ $[M+H]^+$ 414.0815, found 414.0809.

6-Chloro-2-(2-(4-iodophenoxy)pyridin-3-yl)-3,8-dimethylquinazolin-4(3*H*)-one (z5). Yield: 48.9%, white powder, mp 187.9–189.3 °C; ^{1}H NMR (400 MHz, $CDCl_3$) δ 8.31 (dd, *J* = 5.0, 1.9 Hz, 1H), 8.14 (d, *J* = 2.4 Hz, 1H), 7.95 (dd, *J* = 7.4, 1.9 Hz, 1H), 7.72 – 7.69 (m, 1H), 7.68 – 7.66 (m, 1H), 7.56 (dd, *J* = 2.4,

0.8 Hz, 1H), 7.23 (dd, *J* = 7.4, 5.0 Hz, 1H), 6.93 – 6.91 (m, 1H), 6.90 – 6.87 (m, 1H), 3.57 (s, 3H), 2.57 (s, 3H). ^{13}C NMR (101 MHz, $CDCl_3$) δ 161.64, 159.58, 152.76, 151.10, 149.22, 144.71, 140.28, 138.66, 138.48, 134.97, 132.51, 123.68, 123.62, 121.76, 120.10, 119.17, 89.22, 32.97, 17.29. HRMS (ESI) *m/z* calcd for $C_{21}H_{15}ClIN_3O_2$ $[M+H]^+$ 503.9970, found 503.9959.

6-Chloro-2-(2-(3,4-dimethylphenoxy)pyridin-3-yl)-3,8-dimethylquinazolin-4(3*H*)-one (z6). Yield: 20.0%, white powder, mp 159.1–161.0 °C; ^{1}H NMR (400 MHz, $CDCl_3$) δ 8.31 (dd, *J* = 5.0, 1.8 Hz, 1H), 8.14 (d, *J* = 2.2 Hz, 1H), 7.92 (dd, *J* = 7.4, 1.9 Hz, 1H), 7.55 (d, *J* = 1.6 Hz, 1H), 7.20 – 7.09 (m, 2H), 6.90 (d, *J* = 2.3 Hz, 1H), 6.85 (dd, *J* = 8.1, 2.4 Hz, 1H), 3.61 (s, 3H), 2.58 (s, 3H), 2.23 (d, *J* = 2.1 Hz, 6H). ^{13}C NMR (101 MHz, $CDCl_3$) δ 161.68, 160.39, 151.58, 150.62, 149.40, 144.80, 140.04, 138.45, 138.18, 134.84, 133.74, 132.32, 130.59, 123.58, 122.46, 121.74, 119.83, 118.61, 118.43, 32.99, 19.96, 19.24, 17.31. HRMS (ESI) *m/z* calcd for $C_{23}H_{21}O_2N_3Cl$ $[M+H]^+$ 406.1317, found 406.1309.

6-Chloro-2-(2-(3-chloro-4-fluorophenoxy)pyridin-3-yl)-3,8-dimethylquinazolin-4(3*H*)-one (z7). Yield: 25.6%, white powder, mp 185.0–186.4 °C; ^{1}H NMR (500 MHz, $CDCl_3$) δ 8.30 (d, *J* = 2.7 Hz, 1H), 8.14 (s, 1H), 7.95 (d, *J* = 7.3 Hz, 1H), 7.56 (s, 1H), 7.49 (d, *J* = 8.7 Hz, 1H), 7.22 (dd, *J* = 7.0, 5.0 Hz, 1H), 7.02 (d, *J* = 8.7 Hz, 2H), 3.57 (s, 3H), 2.57 (s, 3H). ^{13}C NMR (101 MHz, $CDCl_3$) δ 161.64, 159.63, 151.90, 151.11, 149.21, 144.71, 140.28, 138.49, 134.97, 132.68, 132.51, 123.93, 123.62, 123.30, 121.76, 120.07, 119.37, 119.15, 118.35, 32.97, 17.29. HRMS (ESI) *m/z* calcd for $C_{21}H_{15}O_2N_3Cl_2$ $[M+H]^+$ 430.0520, found 430.0515.

6-Chloro-2-(2-(3,5-dimethylphenoxy)pyridin-3-yl)-3,8-dimethylquinazolin-4(3*H*)-one (z8). Yield: 39.4%, light brown crystals, mp 202.1–203.1 °C; ^{1}H NMR (400 MHz, $CDCl_3$) δ 8.35 (dd, *J* = 5.0, 1.9 Hz, 1H), 8.16 (d, *J* = 2.4 Hz, 1H), 7.95 (dd, *J* = 7.4, 1.9 Hz, 1H), 7.58 (dd, *J* = 2.4, 0.8 Hz, 1H), 7.20 (dd, *J* = 7.4, 5.0 Hz, 1H), 6.86 (s, 1H), 6.76 (s, 2H), 3.63 (s, 3H), 2.60 (s, 3H), 2.32 (s, 6H). ^{13}C NMR (101 MHz, $CDCl_3$) δ 161.71, 160.29, 152.81, 151.58, 149.47, 144.85, 140.07, 139.55, 138.52, 134.89, 132.38, 127.28, 123.63, 121.79, 120.07, 119.03, 118.58, 33.05, 21.36, 17.35. HRMS (ESI) *m/z* calcd for $C_{23}H_{21}O_2N_3Cl$ $[M+H]^+$ 406.1317, found 406.1310.

6-Chloro-3,8-dimethyl-2-(2-(3-(trifluoromethyl)phenoxy)pyridin-3-yl)quinazolin-4(3*H*)-one (z9). Yield: 46.5%, white powder, mp 142.3–143.8 °C; ^{1}H NMR (500 MHz, $CDCl_3$) δ 8.31 (dd, *J* = 5.0, 1.9 Hz, 1H), 8.14 (d, *J* = 2.0 Hz, 1H), 7.97 (dd, *J* = 7.4, 1.9 Hz, 1H), 7.56 (dd, *J* = 2.4, 0.8 Hz, 1H), 7.51 (t, *J* = 7.9 Hz, 1H), 7.47 (d, *J* = 7.8 Hz, 1H), 7.40 (s, 1H), 7.33 (d, *J* = 7.9 Hz, 1H), 7.25 (dd, *J* = 7.3, 5.1 Hz, 1H), 3.59 (s, 3H), 2.57 (s, 3H). ^{13}C NMR (126 MHz, $CDCl_3$) δ 161.73, 159.48, 153.17, 151.05, 149.32, 144.80, 140.46, 138.63, 135.09, 132.66, 132.34, 130.28, 125.06, 123.72, 122.16, 121.88, 120.35, 119.58, 118.79, 67.18, 33.11, 17.36. HRMS (ESI) *m/z* calcd for $C_{22}H_{16}O_2N_3ClF_3$ $[M+H]^+$ 446.0878, found 446.0871.

6-Chloro-2-(2-(3-fluorophenoxy)pyridin-3-yl)-3,8-dimethylquinazolin-4(3*H*)-one (z10). Yield: 51.6%, white solid, mp 142.3–143.8 °C; ^{1}H NMR (500 MHz, $CDCl_3$) δ 8.32 (tt, *J* = 6.5, 3.2 Hz, 1H), 8.14 (dd, *J*

= 7.2, 3.4 Hz, 1H), 8.00 – 7.91 (m, 1H), 7.65 – 7.47 (m, 1H), 7.39 – 7.30 (m, 1H), 7.24 (ddd, *J* = 9.3, 6.4, 4.6 Hz, 1H), 6.98 – 6.84 (m, 3H), 3.61 – 3.55 (m, 3H), 2.60 – 2.53 (m, 3H). ^{13}C NMR (101 MHz, $CDCl_3$) δ 164.34, 161.64, 159.52, 153.86, 151.10, 149.30, 144.73, 140.32, 138.54, 134.96, 132.51, 130.36, 123.62, 121.78, 120.25, 119.34, 117.12, 112.47, 109.57, 33.00, 17.29. HRMS (ESI) *m/z* calcd for $C_{21}H_{16}O_2N_3ClF$ $[M+H]^+$ 396.0910, found 396.0903.

6-Chloro-2-(2-(4-chloro-3-methylphenoxy)pyridin-3-yl)-3,8-dimethylquinazolin-4(3*H*)-one (z11). Yield: 23.5%, white powder, mp 150.5–151.3 °C; ^{1}H NMR (400 MHz, $CDCl_3$) δ 8.34 (dd, *J* = 5.0, 1.9 Hz, 1H), 8.17 (d, *J* = 3.0 Hz, 1H), 7.96 (dd, *J* = 7.4, 2.0 Hz, 1H), 7.59 (dd, *J* = 2.5, 0.8 Hz, 1H), 7.36 (d, *J* = 8.6 Hz, 1H), 7.23 (dd, *J* = 7.4, 5.0 Hz, 1H), 7.03 (d, *J* = 2.6 Hz, 1H), 6.94 (dd, *J* = 8.6, 3.3 Hz, 1H), 3.60 (s, 3H), 2.60 (s, 3H), 2.37 (s, 3H). ^{13}C NMR (101 MHz, $CDCl_3$) δ 161.67, 159.88, 151.25, 151.18, 149.31, 144.77, 140.26, 138.51, 137.69, 134.96, 132.49, 130.90, 129.98, 123.87, 123.63, 121.78, 120.24, 120.06, 119.01, 33.00, 20.30, 17.31. HRMS (ESI) *m/z* calcd for $C_{22}H_{18}O_2N_3Cl_2$ $[M+H]^+$ 426.0771, found 426.0765.

6-Chloro-2-(2-(2-fluorophenoxy)pyridin-3-yl)-3,8-dimethylquinazolin-4(3*H*)-one (z12). Yield: 48.4%, white powder, mp 200.0–201.4 °C; ^{1}H NMR (500 MHz, $CDCl_3$) δ 8.27 (dd, *J* = 5.0, 1.9 Hz, 1H), 8.14 (d, *J* = 1.8 Hz, 1H), 7.94 (dd, *J* = 7.4, 1.9 Hz, 1H), 7.55 (dd, *J* = 2.4, 0.9 Hz, 1H), 7.25 – 7.14 (m, 5H), 3.60 (s, 3H), 2.58 (s, 3H). ^{13}C NMR (101 MHz, $CDCl_3$) δ 161.62, 159.29; 151.64; 150.87; 149.22; 144.69; 140.43; 138.55; 135.03; 133.16; 132.61; 130.92; 129.16; 123.77; 123.64; 121.78; 121.20; 120.17; 119.59; 33.01; 17.31. HRMS (ESI) calcd for $C_{21}H_{16}O_2N_3ClF$ $[M+H]^+$ 396.0910, found 396.0903.

6-Chloro-2-(2-(3-bromophenoxy)pyridin-3-yl)-3,8-dimethylquinazolin-4(3*H*)-one (z13). Yield: 44.2%, white powder, mp 135.0–136.8 °C; ^{1}H NMR (400 MHz, $CDCl_3$) δ 8.33 (dd, *J* = 5.0, 1.9 Hz, 1H), 8.14 (d, *J* = 2.3 Hz, 1H), 7.96 (dd, *J* = 7.4, 1.9 Hz, 1H), 7.56 (d, *J* = 1.7 Hz, 1H), 7.37 – 7.29 (m, 2H), 7.27 (t, *J* = 3.6 Hz, 1H), 7.24 (t, *J* = 3.7 Hz, 1H), 7.08 (dd, *J* = 8.1, 1.3 Hz, 1H), 3.58 (s, 3H), 2.57 (s, 3H). ^{13}C NMR (101 MHz, $CDCl_3$) δ 161.62, 159.48, 153.46, 151.02, 149.26, 144.69, 140.28, 138.51, 134.95, 132.50, 130.67, 128.48, 124.86, 123.60, 122.60, 121.74, 120.23, 120.14, 119.32, 32.99, 17.29. HRMS (ESI) *m/z* calcd for $C_{21}H_{16}O_2N_3BrCl$ $[M+H]^+$ 456.0109, found 456.0101.

6-Chloro-2-(2-(4-fluoro-2-methylphenoxy)pyridin-3-yl)-3,8-dimethylquinazolin-4(3*H*)-one (z14). Yield: 55.6%, white powder, mp 189.2–190.4 °C; ^{1}H NMR (400 MHz, $CDCl_3$) δ 8.29 (dd, *J* = 5.0, 1.9 Hz, 1H), 8.15 (d, *J* = 2.3 Hz, 1H), 7.91 (dd, *J* = 7.4, 1.9 Hz, 1H), 7.57 (dd, *J* = 2.4, 0.7 Hz, 1H), 7.19 (dd, *J* = 7.4, 5.0 Hz, 1H), 7.00 (dt, *J* = 10.0, 5.0 Hz, 1H), 6.97 – 6.93 (m, 1H), 6.90 (dd, *J* = 8.4, 3.0 Hz, 1H), 3.60 (s, 3H), 2.58 (s, 3H), 2.11 (s, 3H). ^{13}C NMR (101 MHz, $CDCl_3$) δ 161.62, 159.29, 151.64, 150.87, 149.22, 144.69, 140.43, 138.55, 135.03, 133.16, 132.61, 130.92, 129.16, 123.77, 123.64, 121.78, 121.20, 120.17, 119.59, 33.01, 17.31. HRMS (ESI) *m/z* calcd for $C_{22}H_{18}O_2N_3ClF$ $[M+H]^+$ 410.1066, found 410.1057.

Anticancer assay

MTT assay

The newly synthesized quinazolinones derivatives were screened for their antitumor activity using 3-(4,5-dimethylthiazol-2-yl)-2,5-diphenyltetrazolium bromide (MTT) assay and the commercial drug Gefitinib was used as the positive control. Briefly, exponentially growing cells (3×10^4 / mL) were plated in 96-well plates and cultured overnight at 37 °C in a 5% CO_2-supplemented atmosphere. Then, cancer cell lines were treated for 48 h with various concentrations of compounds from 0.625 to 10 μM. Next, 20 μL of MTT (5 mg/mL) was added to each well and incubated continually for 4 h at 37 °C. Then, the culture medium was removed, and the formazan crystals were dissolved in 150 μL DMSO for each well and shook for 10−15 min. Finally, the absorbance of each well was measured at 490 nm (Abs) by TW 200 PRO (Enzyme-labelled meter). All measurements were performed in three times and had triplicate samples in each time. Error bars were calculated from standard deviation from the mean and the IC_{50} were analyzed by the Graphpad Prism software package.

Scratch wound assay

Cell migration is a central and integral process of various important biological mechanisms like tissue development, tissue wound healing and pathological conditions like cancer. Uncontrolled cell migration is the first step and hallmark of cancer cell metastasis. Effect of **z8** on A549 cell migration was determined by scratch wound assay. Firstly, cells were seeded at a density of 1×10^5 / mL in a 6 well plate. The following day, artificial wound was created by disrupting monolayer of cells with a sterile 10 μL tip across the centre of the well. Then, washed each well with sterile PBS to remove detached cells and fresh culture media supplemented with 1% FBS was added. Next, the cells were treated with **z8** at doses of 5, 10, 20 and 30 μM accordingly. Representative photographs of the artificially created gap were captured by camera (Nikon Ti-S Inverted fluorescence microscope) at 0, 12, 24, 48 h post incubation and were evaluated using image J.

DAPI staining

4,6-Diamidino-2-phenylindole (DAPI) is a fluorescent dye which specifically binds to adenine-thymine clusters of double stranded DNA and stains it blue. Healthy cells display intact round nuclei with distinct margins upon staining with DAPI, where as apoptotic cells show intense blue fluorescence as compared to nuclei of healthy cells. Additionally, condensed chromosome and nuclear fragmentation are apparent in apoptotic cells. The cells in the logarithmic phase were seeded in 6-well plates, and growing cells (1×10^5 / mL) were plated in 6-well plates and cultured overnight at 37 °C in a 5% CO_2 supplemented atmosphere, and then treated with various concentrations of the test compounds for 48 h. Then washed each well with PBS. Added 0.5 mL of 4% cell tissue fixative solution for 15 min. Finally, added 0.5 mL 10 μg/mL DAPI staining solution for 10−15 min in the dark. Representative images for nuclear morphological changes

induced by **z8** were captured by inverted fluorescence microscope (Nikon, Ti-S) using 20× objective lens and were evaluated using image J.

ACKNOWLEDGEMENTS

This work was supported by the State Key Laboratory of Functions and Applications of Medicinal Plants (No. FAMP201707K), State Key Laboratory of Functions and Applications of Medicinal Plants (No. FAMP201801K) and Guizhou Provincial Natural Science Foundation (No. 20181051).

REFERENCES

1. R. L. Siegel, K. D. Miller, and A. Jemal, *Ca-Cancer J. Clin.*, 2019, **69**, 7.
2. G. Schwartsmann, B. Winograd, and H. M. Pinedo, *Radiother. Oncol.*, 1988, **12**, 301.
3. S. Gatadi, G. Pulivendala, J. Gour, S. Malasala, S. Bujji, R. Parupalli, M. Shaikh, C. Godugu, and S. Nanduri, *J. Mol. Struct.*, 2020, **1200**, 127097.
4. H. Q. Wei, Y. Q. Duan, W. F. Gou, J. Cui, H. X. Ning, D. J. Li, Y. Qin, Q. Liu, and Y. L. Li, *Eur. J. Med. Chem.*, 2019, **181**, 111552.
5. D. Li, L. Ambrogio, T. Shimamura, S. Kubo, M. Takahashi, L. R. Chirieac, R. F. Padera, G. I. Shapiro, A. Baum, F. Himmelsbach, W. J. Rettig, M. Meyerson, F. Solca, H. Greulich, and K. K. Wong, *Oncogene*, 2008, **27**, 4702.
6. D. Das, L. Z. Xie, J. B. Wang, X. Xu, Z. H. Zhang, J. L. Shi, X. Y. Le, and J. Hong, *Bioorg. Med. Chem. Lett.*, 2019, **29**, 591.
7. R. Newton, K. A. Bowler, E. M. Burns, P. J. Chapman, E. E. Fairweather, S. J. R. Fritzl, K. M. Goldberg, N. M. Hamilton, S. V. Holt, G. V. Hopkins, S. D. Jones, A. M. Jordan, A. J. Lyons, H. Nikki March, N. Q. McDonald, L. A. Maguire, D. P. Mould, A. G. Purkiss, H. F. Small, A. I. J. Stowell, G. J. Thomson, I. D. Waddell, B. Waszkowycz, A. J. Watson, and D. J. Ogilvie, *Eur. J. Med. Chem.*, 2016, **112**, 20.
8. A. M. Jordan, H. Begum, E. Fairweather, S. Fritzl, K. Goldberg, G. V. Hopkins, N. M. Hamilton, A. J. Lyons, H. N. March, R. Newton, H. F. Small, S. Vishwanath, I. D. Waddell, B. Waszkowycz, A. J. Watson, and D. J. Ogilvie, *Bioorg. Med. Chem. Lett.*, 2016, **26**, 2724.
9. M. Xin, Y. Y. Hei, H. Zhang, Y. Shen, and S. Q. Zhang, *Bioorg. Med. Chem. Lett.*, 2017, **27**, 1972.
10. H. W. Ding, C. L. Deng, D. D. Li, D. D. Liu, S. M. Chai, W. Wang, Y. Zhang, K. Chen, X. Li, J. Wang, S. J. Song, and H. R. Song, *Eur. J. Med. Chem.*, 2018, **146**, 460.
11. K. P. Rakesh, H. K. Kumara, H. M. Manukumar, and D. Channe Gowda, *Bioorg. Chem.*, 2019, **87**, 252.
12. X. D. Ma, F. Fang, Q. Q. Tao, L. Shen, G. C. Zhong, T. Qiao, X. Q. Lv, and J. M. Li,

MedChemComm, 2019, **10**, 413.

13. D. Bhattarai, J. H. Jung, S. Han, H. Lee, S. J. Oh, H. W. Ko, and K. Lee, *Eur. J. Med. Chem.*, 2017, **125**, 1036.
14. L. H. Shao, Y. Y. Gan, M. Hou, S. L. Tao, L. Q. Zhang, Z. C. Wang, and G. P. Ouyang, *Chin. J. Org. Chem.*, 2020, **40**, 1.
15. Y. Le, Y. Y. Gan, Y. H. Fu, J. M. Liu, W. Li, X. Zou, Z. X. Zhou, Z. C. Wang, G. P. Ouyang, and L. J. Yan, *J. Enzyme Inhib. Med. Chem.*, 2020, **35**, 555.
16. Y. B. Wang, S. C. Zheng, Y. M. Hu, and B. Tan, *Nat. Commun.*, 2017, **8**, 15489.
17. J. G. Zhou and J. Fang, *J. Org. Chem.*, 2011, **76**, 7730.
18. H. Hikawa, Y. Ino, H. Suzuki, and Y. Yokoyama, *J. Org. Chem.*, 2012, **77**, 7046.
19. W. Xu, Y. B. Jin, H. X. Liu, Y. Y. Jiang, and H. Fu, *Org. Lett.*, 2011, **13**, 1274.
20. T. Kotipalli, V. Kavala, D. Janreddy, V. Bandi, C. W. Kuo, and C. F. Yao, *Eur. J. Org. Chem.*, 2016, 1182.
21. T. Abe, K. Kida, and K. Yamada, *Chem. Commun.*, 2017, **53**, 4362.
22. M. R. Yadav, S. T. Shirude, A. Parmar, R. Balaraman, and R. Giridhar, *Chem. Heterocycl. Compd.*, 2006, **42**, 1038.
23. K. Kloc, I. Maliszewska, and J. Młochowski, *Synth. Commun.*, 2003, **33**, 3805.